Journal of Statistical Physics, Vol. 25, No. 3, 1981

A Seven-Mode Truncation of the Plane Incompressible Navier–Stokes Equations

Valter Franceschini[1] and Claudio Tebaldi[2]

Received May 30, 1980

A model obtained by a seven-mode truncation of the Navier–Stokes equations for a two-dimensional incompressible fluid on a torus is studied. This model, extending a previously studied five-mode one, exhibits a very rich and varied phenomenology including some remarkable properties of hysteresis (i.e., coexistence of attractors). A stochastic behavior is found for high values of the Reynolds number, when no stable fixed points, closed orbits, or tori are present.

KEY WORDS: Navier–Stokes equations; turbulence; strange attractors; periodic orbits; Poincaré map.

1. INTRODUCTION

In the line of studying simple nonlinear evolution equations which, although deterministic, exhibit a stochastic ("turbulent") behavior when some parameters go beyond certain critical values, a model with interesting properties has been proposed in Ref. 1 and studied in more detail in Ref. 2. Such a model, consisting of five first-order ordinary differential equations, is obtained by a suitable five-mode truncation of the Navier–Stokes equations for a two-dimensional incompressible fluid on a torus. The most remarkable features shown by a careful numerical investigation are the following:

(a) In a certain interval $[r_1, r_2]$ of the Reynolds number r, the system has a stochastic behavior which, as predicted by Ruelle and Takens in Ref. 3, appears due to the presence of strange attractors (in our case two and symmetrically placed).

[1] Istituto di Matematica, Università di Modena, Modena, Italy.
[2] Istituto di Matematica Applicata and Istituto di Fisica, Università di Bologna, Bologna, Italy.

0022-4715/81/0700-0397$03.00/0

(b) For $r < r_1$ the system exhibits two different sequences of infinite bifurcations: a closed periodic orbit becomes unstable and a new stable one, with a doubled period, arises at every bifurcation. The two sequences are found to be strictly related to the generation of the strange attractors at $r = r_1$.

(c) The two strange attractors disappear at $r = r_2$, the turbulent behavior giving place to periodic motion, persistent with r increasing towards infinity. The disappearance of each strange attractor occurs because of the simultaneous arising of two "twin" orbits, one stable and the other unstable. The periodic behavior shown for $r > r_2$ is in fact due to such a stable orbit.

The features described seem relevant to the understanding of the mechanism by which turbulence can develop. They are closely analogous to those of the Lorenz model,[4–6] the starting point of recent attempts at a mathematical interpretation of turbulence.

An obvious and quite relevant question about any kind of highly truncated models of systems having in reality infinite degrees of freedom is how truncation affects the phenomenology exhibited by the model. In this work we consider an extension of the model studied in Refs. 1 and 2, obtained by truncation of the Navier–Stokes equations to seven modes, two new ones having been added to the previous five. Our purpose is to study how the phenomenology of the model changes when the number of modes in the truncation is slightly increased. By adding two modes only, one could hope that the qualitative properties of the five-mode model could persist to some extent also in the larger one. This is, however, not the case: in the larger model neither is a sequence of infinite bifurcating periodic orbits present nor does a stable attracting periodic orbit exist at high values of the Reynolds number R. Turbulence is now present at high R and is reached through a quite different phenomenology.[3]

Our results are rather analogous to what is found by Curry in Ref. 7, where a 14-mode extension of the Lorenz model is studied. In fact, while in the Lorenz system the strange attractor arises via a subcritical Hopf bifurcation, in the generalized one turbulence is reached when, after a few bifurcations starting from a direct Hopf bifurcation, two symmetrically placed tori become unstable. Moreover, also in the generalized Lorenz model, no sequence of infinite bifurcations is found as well as no stable attracting periodic orbit being present at high values of the Rayleigh number.

Even if the seven-mode model studied does not reproduce the interest-

[3] A study is in progress on a system $\dot{\mathbf{x}} = \mathbf{F}(\mathbf{x}, R, \epsilon)$ representing a continuous transition from the five-mode model to the seven-mode one as ϵ varies from 0 to 1.

ing phenomena of the five-mode one, we think it is also interesting by itself. In fact its phenomenology, studied quite in detail, appears so rich and varied to amply justify the present work.

2. THE MODEL

Consider the incompressible Navier–Stokes equations on the torus $T^2 = [0, 2\pi] \times [0, 2\pi]$:

$$\frac{\partial \mathbf{u}}{\partial t} + (\mathbf{u} \cdot \nabla)\mathbf{u} = -\nabla p + \mathbf{f} + \nu \Delta \mathbf{u}$$

$$\operatorname{div} \mathbf{u} = 0$$

$$\int_{T^2} \mathbf{u}\, d\mathbf{x} = \mathbf{0}$$

where $\mathbf{u}$ is the velocity field, p is the pressure, and $\mathbf{f}$ is a periodic volume force.

We expand $\mathbf{u}$ in Fourier series

$$\mathbf{u}(\mathbf{x}) = \sum_{\mathbf{k} \neq \mathbf{0}} \exp(i\mathbf{k} \cdot \mathbf{x}) \gamma_{\mathbf{k}} \frac{\mathbf{k}^{\perp}}{|\mathbf{k}|}$$

where $\mathbf{k} = (h_1, h_2)$ is a "wave vector" with integer components, $\mathbf{k}^{\perp} = (h_2, -h_1)$ and the reality condition $\gamma_{\mathbf{k}} = -\bar{\gamma}_{-\mathbf{k}}$ must hold. Considering the analogous expansions for p and $\mathbf{f}$ and a finite set L of wave vectors such that if $\mathbf{k} \in L$ also $-\mathbf{k} \in L$, we obtain the truncated Navier–Stokes equations:

$$\dot{\gamma}_{\mathbf{k}} = i \sum_{\substack{\mathbf{k}_1 + \mathbf{k}_2 + \mathbf{k} = 0 \\ \mathbf{k}_1, \mathbf{k}_2 \in L}} \frac{(\mathbf{k}_1^{\perp} \cdot \mathbf{k}_2)(k_2^2 - k_1^2)}{2|\mathbf{k}_1|\,|\mathbf{k}_2|\,|\mathbf{k}|} \bar{\gamma}_{\mathbf{k}_1} \bar{\gamma}_{\mathbf{k}_2} - \nu |\mathbf{k}|^2 \gamma_{\mathbf{k}} + f_{\mathbf{k}} \tag{2.1}$$

$$\gamma_{\mathbf{k}} = -\bar{\gamma}_{-\mathbf{k}} \qquad (\mathbf{k} \in L)$$

$f_{\mathbf{k}}$ being the component of $\mathbf{f}$ with respect to $\exp(i\mathbf{k} \cdot \mathbf{x})(\mathbf{k}^{\perp}/|\mathbf{k}|)$.

In this paper we take L as the set of vectors $\mathbf{k}_1 = (1, 1)$, $\mathbf{k}_2 = (3, 0)$, $\mathbf{k}_3 = (2, -1)$, $\mathbf{k}_4 = (1, 2)$, $\mathbf{k}_5 = (0, 1)$, $\mathbf{k}_6 = (1, 0)$, $\mathbf{k}_7 = (1, -2)$ and their opposites (Fig. 1). Since with this choice of L equations (2.1) also admit solutions in which each component $\gamma_{\mathbf{k}_i}$ is either real or purely imaginary, we can consider the following solution: $\gamma_{\mathbf{k}_1} = x_1$, $\gamma_{\mathbf{k}_2} = -ix_2$, $\gamma_{\mathbf{k}_3} = x_3$, $\gamma_{\mathbf{k}_4} = ix_4$, $\gamma_{\mathbf{k}_5} = x_5$, $\gamma_{\mathbf{k}_6} = ix_6$, $\gamma_{\mathbf{k}_7} = ix_7$, with real x_i's.

After suitable changes in time and length scales in order to have $\nu = 1$ and to get rid of some factors, and assuming a force $\mathbf{f}$ acting only on the

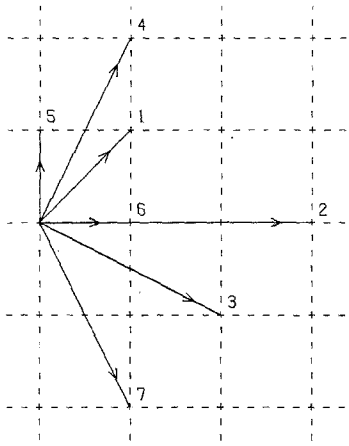

Fig. 1. Representation of the vectors $\mathbf{k}_i$, $i = 1, \ldots, 7$, which with their opposites constitute the set L.

mode $\mathbf{k}_3$, equations (2.1) give

$$\begin{aligned}
\dot{x}_1 &= -2x_1 + 4\sqrt{5}\, x_2x_3 + 4\sqrt{5}\, x_4x_5 \\
\dot{x}_2 &= -9x_2 + 3\sqrt{5}\, x_1x_3 \\
\dot{x}_3 &= -5x_3 - 7\sqrt{5}\, x_1x_2 + 9x_1x_7 + R \\
\dot{x}_4 &= -5x_4 - \sqrt{5}\, x_1x_5 \\
\dot{x}_5 &= -x_5 - 3\sqrt{5}\, x_1x_4 + 5x_1x_6 \\
\dot{x}_6 &= -x_6 - 5x_1x_5 \\
\dot{x}_7 &= -5x_7 - 9x_1x_3
\end{aligned} \tag{2.2}$$

where R is our Reynolds number.

Since the modes $\mathbf{k}_i$, $i = 1, \ldots, 5$, are the ones used for truncation in Ref. 1, the system (2.2) is an extension of the five-mode model proposed there. In fact if we let $x_i = \gamma_i/\sqrt{5}$, $i = 1, \ldots, 5$, $x_6 = x_7 = 0$, $R = r/\sqrt{5}$, the first five equations give the system (2.4) of Ref. 1.

We remark that the system (2.2) has the three following symmetries:

$$\begin{aligned}
&(\alpha) \qquad (x_1, x_2, x_3, -x_4, -x_5, -x_6, x_7) \Leftrightarrow (x_1, x_2, x_3, x_4, x_5, x_6, x_7) \\
&(\beta) \quad (-x_1, -x_2, x_3, -x_4, x_5, -x_6, -x_7) \Leftrightarrow (x_1, x_2, x_3, x_4, x_5, x_6, x_7) \\
&(\gamma) \qquad (-x_1, -x_2, x_3, x_4, -x_5, x_6, -x_7) \Leftrightarrow (x_1, x_2, x_3, x_4, x_5, x_6, x_7)
\end{aligned}$$

which form a group together with the identity transformation.

3. FIXED POINTS AND THEIR STABILITY

The model (2.2) has the following stationary properties:

(a) For $0 < R \leqslant R_1 = (15/2)^{1/2}$ there is only one fixed point P_0, with components $x_1 = x_2 = x_4 = x_5 = x_6 = x_7 = 0$, $x_3 = R/5$. It is stable and, by numerical evidence, globally attractive. This result is in agreement with the general theory on stability of the solutions for the Navier–Stokes equations,[8] which predicts such a behavior for R sufficiently small, and reproduces the exact behavior of the five-mode model.

(b) For $R_1 < R \leqslant R_2 = R_1 + (3762/25\sqrt{30}) \simeq 30.2124$ three fixed points are present: the previous one P_0, which has become unstable since one of the eigenvalues of the Liapunov matrix has crossed the imaginary axis at $R = R_1$, and two more, P_+ and P_-, bifurcated from P_0, with components

$$x_1 = \pm 5\sqrt{6}\left(\frac{2R - \sqrt{30}}{836\sqrt{30}}\right)^{1/2}$$

$$x_2 = \pm 5\left(\frac{2R - \sqrt{30}}{836\sqrt{30}}\right)^{1/2}$$

$$x_3 = (3/10)^{1/2}$$

$$x_4 = x_5 = x_6 = 0$$

$$x_7 = \mp \frac{27}{\sqrt{5}}\left(\frac{2R - \sqrt{30}}{836\sqrt{30}}\right)^{1/2}$$

They are stable and attracting: any randomly chosen initial point goes either to P_+ or to P_-. At $R = R_2$ a pair of complex conjugate eigenvalues of the Liapunov matrix in $P_\pm$ crosses the imaginary axis, their real part becoming positive, so that we have the following.

(c) For $R > R_2$ all the fixed points of (2.2) are unstable.

4. PERIODIC AND QUASIPERIODIC SOLUTIONS

For $R_2 < R < R_{12} \simeq 248.2$ the model exhibits a rather complicated behavior, with several periodic and quasiperiodic solutions, often present at the same time and for rather large ranges of the parameter. For a clear exposition of all the phenomenology, it appears natural to present it divided into four parts, each of them related to one of the four different periodic orbits which we have found.

4.1. Orbits $\mathcal{Q}$, TORI $T(\mathcal{Q})$

At $R = R_2$, from the points P_+ and P_-, two symmetric orbits $\mathcal{Q}_+$ and $\mathcal{Q}_-$ (Fig. 2) arise via a direct Hopf bifurcation, each one invariant under the symmetry (α) and transformed in the other one by (β) or (γ). It is easy to verify that, as predicted by the Hopf theorem (see, for example, Ref. 3), the period of such orbits tends to $T = (2\pi/|\gamma_0|) \simeq 1.167$ for $R \to R_2$ from above, γ_0 being the imaginary part of the two eigenvalues crossing the imaginary axis. The orbits $\mathcal{Q}$ remain stable and attracting up to $R = R_4 \simeq 71.30$, becoming unstable because a pair of complex conjugate eigenvalues of the Liapunov matrix for the Poincaré map crosses the unit circle. Again numerical evidence shows agreement with the predictions of the bifurcation theory[3]: two attracting tori $T(\mathcal{Q}_+)$ and $T(\mathcal{Q}_-)$ arise from the two orbits $\mathcal{Q}_+$ and $\mathcal{Q}_-$.

Figure 3 provides a plane projection of the motion of a randomly chosen initial point on a torus $T(\mathcal{Q})$ for two values of the parameter, $R = 71.40$ and $R = 72$. Two facts appear evident looking at the figures: (i) each torus $T(\mathcal{Q})$ rapidly grows as R increases; (ii) every point which goes over a torus $T(\mathcal{Q})$ describes trajectories which seem to possess all the characteristics of the ones of a quasiperiodic motion. These facts can be further supported studying the behavior of the flow in a neighborhood of an orbit $\mathcal{Q}$, a little later than it has become unstable. In order to make such a study we have defined a Poincaré map considering a hyperplane Π

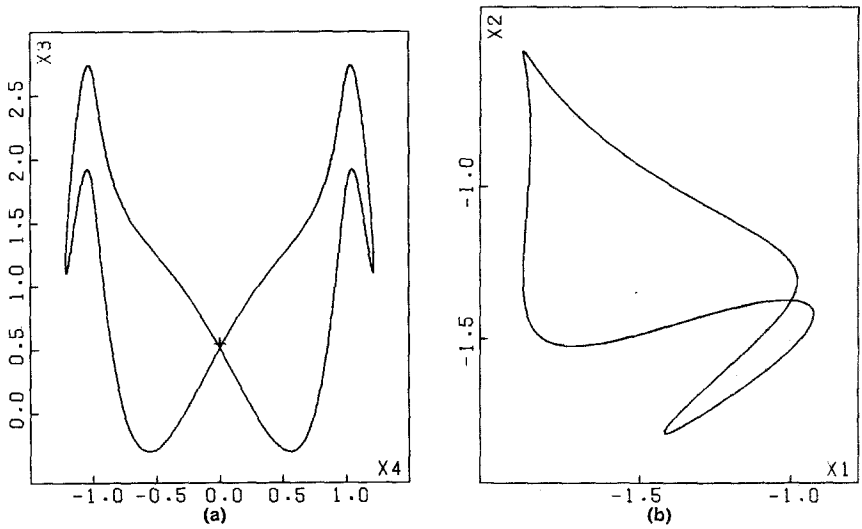

Fig. 2. Projections of the stable orbit $\mathcal{Q}_-$ for $R = 71$. The symbol + represents the fixed points $P_\pm$.

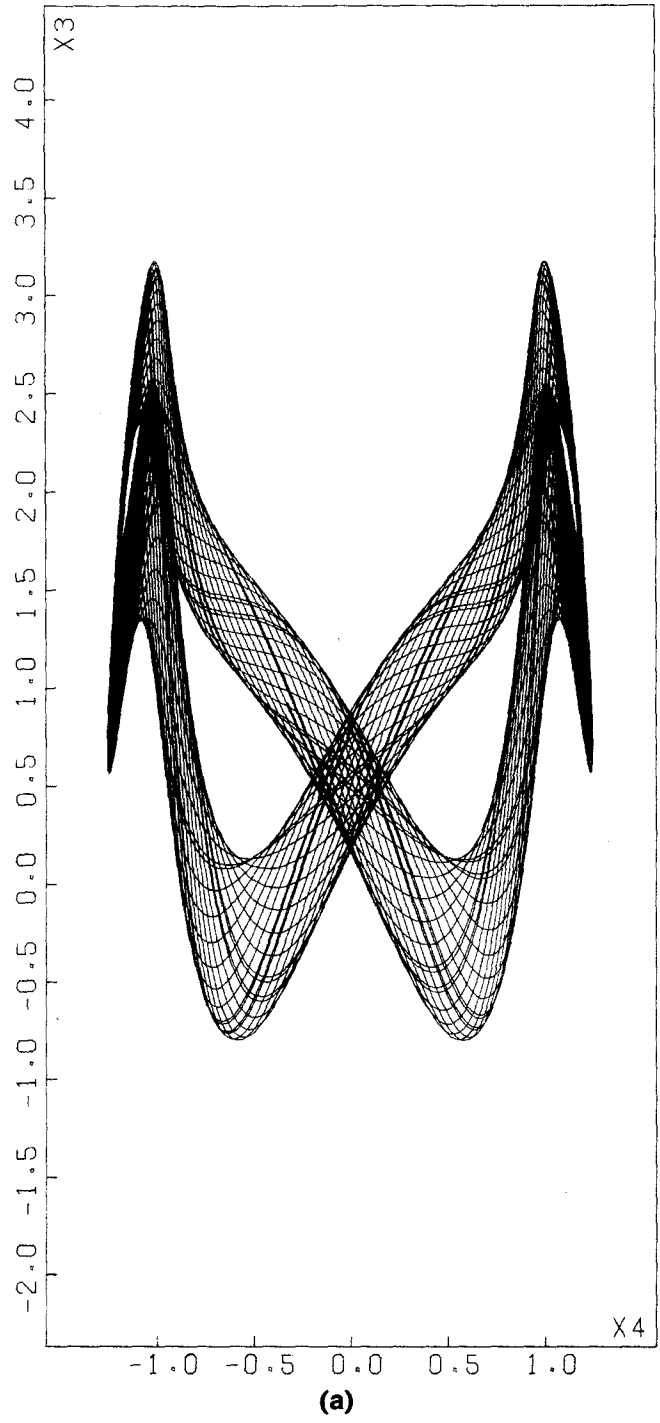

Fig. 3. Projections of the flow on a torus $T(\mathcal{C})$ for $R =$ (a) 71.40; (b) 72.00.

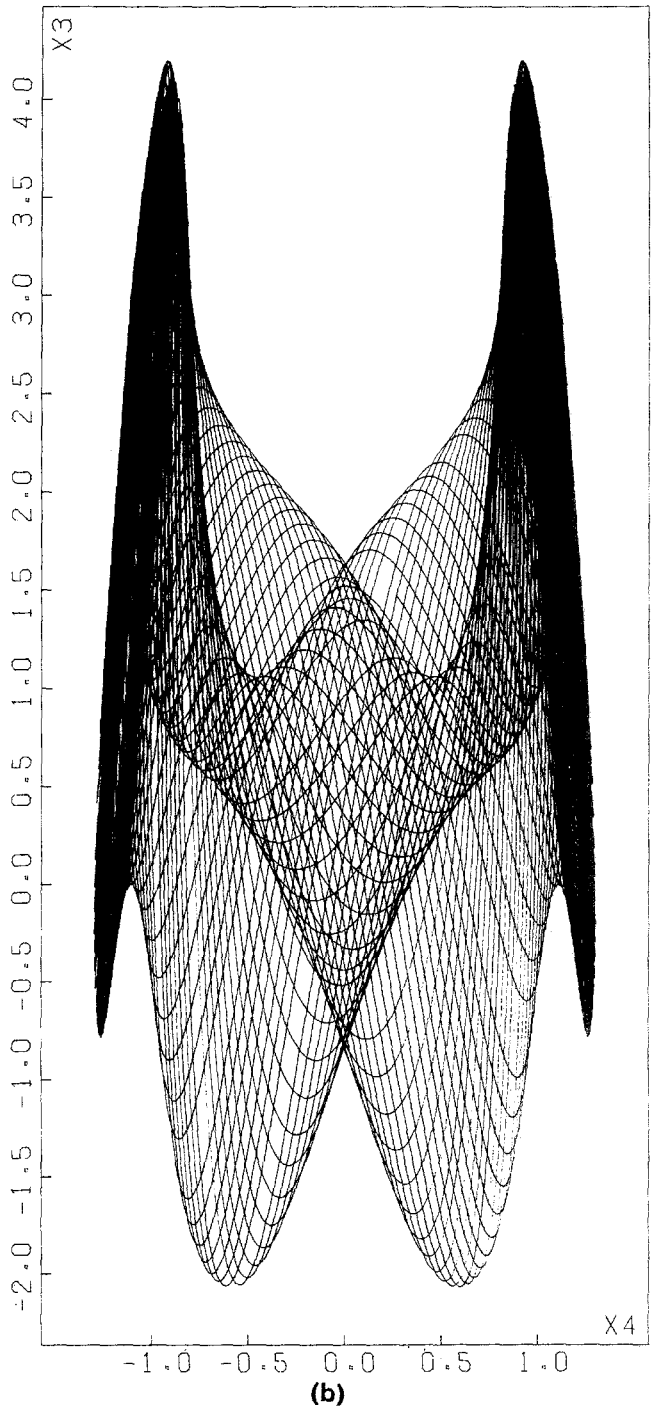

(b)

Fig. 3. Continued.

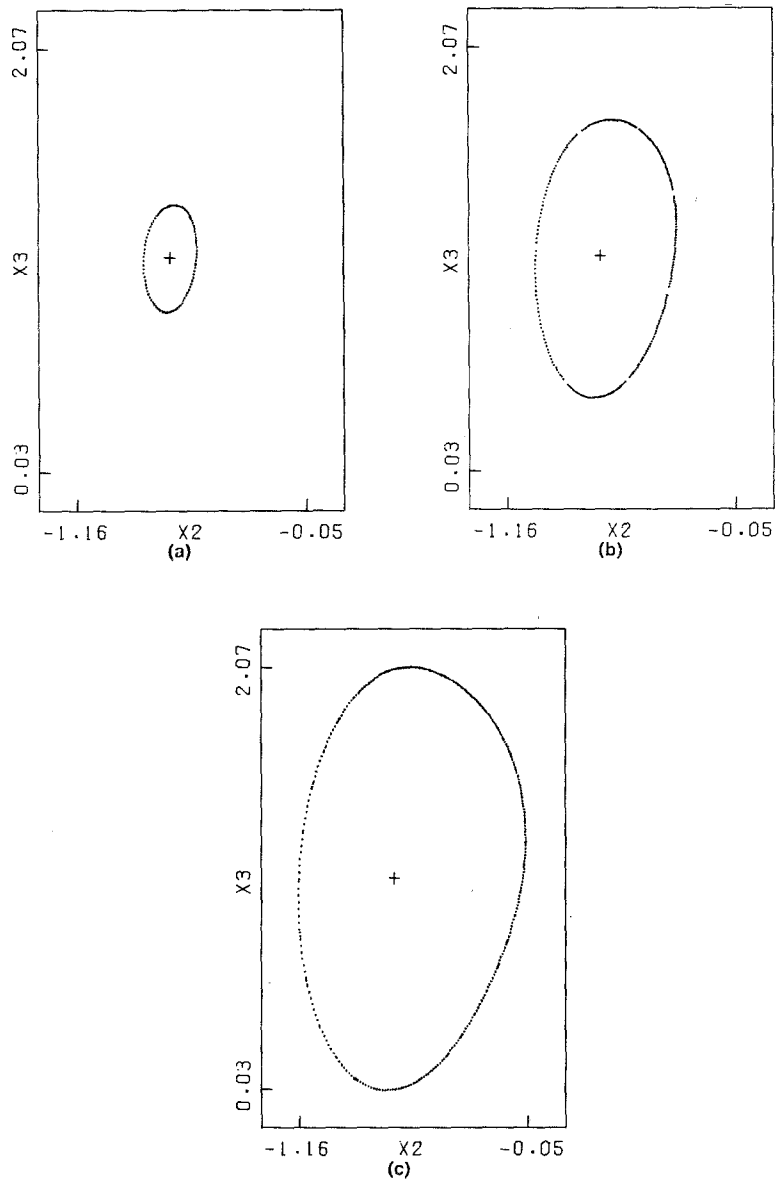

Fig. 4. Projections of the Poincaré map for the flow on a torus T on a hyperplane normal to $\mathcal{C}$ at a conveniently chosen point for $R =$ (a) 71.40 (100 intersections); (b) 71.80 (250 intersections); (c) 72.10 (350 intersections).

normal to $\mathcal{C}$ at a conveniently chosen point P, and then observing the intersections of the solution curve with a suitable portion σ of Π containing P. Figure 4 provides the projection of σ in the plane (x_2, x_3) for $R = 71.40$, $R = 71.80$, and $R = 72.10$, showing the intersections of the flow with our codimension-1 section. Such figure gives very strong evidence that in R_4 a direct bifurcation to a torus has taken place, clearly confirming our previous statements.

For $R > R_5 \simeq 72.11$ the two tori $T(\mathcal{C})$ do not attract any more. Every point, randomly chosen in a neighborhood of an orbit $\mathcal{C}$, stays there for a short time only and afterwards goes rapidly to one of the two stable orbits $\mathcal{B}$ (see below).

4.2. ORBITS $\mathcal{B}$, TORI $T(\mathcal{B})$

For $63.30 \simeq R_3 < R < R_{10} \simeq 192.75$ two symmetric orbits $\mathcal{B}_1$ and $\mathcal{B}_2$ (Fig. 5), stable and attracting, are present, each one invariant under the symmetry (β) and changed in the other by (α) or (γ). The study of the stability properties of these two orbits shows that they lose stability both in R_3 and R_{10} because a pair of complex conjugate eigenvalues crosses the unit circle. Let us consider first the bifurcation in R_{10}. As in R_4 for the orbits $\mathcal{C}$, we have strong numerical evidence of a bifurcation to an invariant attracting torus. Each orbit $\mathcal{B}$ gives rise to a torus $T(\mathcal{B})$, growing as R increases and attracting up to $R = R_{11} \simeq 227.1$. Any randomly chosen

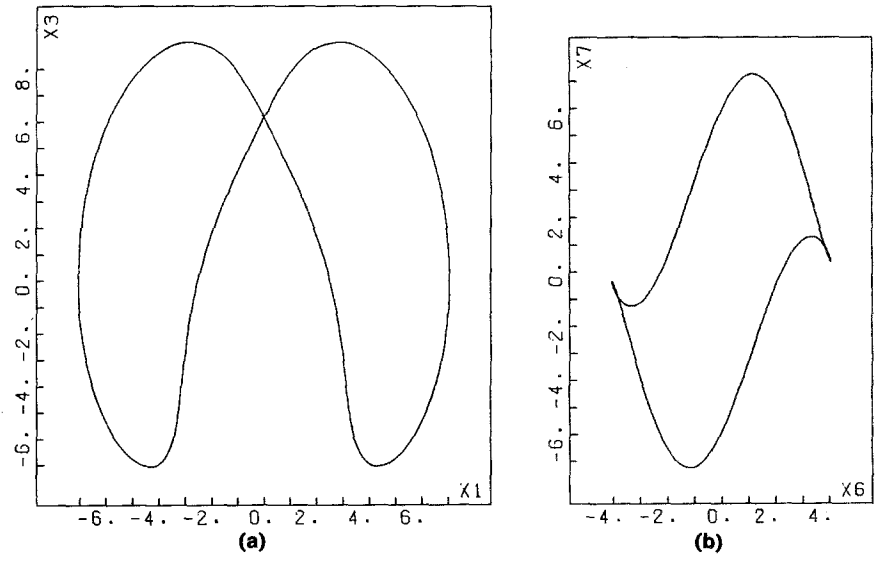

Fig. 5. Projections of a stable orbit $\mathcal{B}$ for $R = 190$.

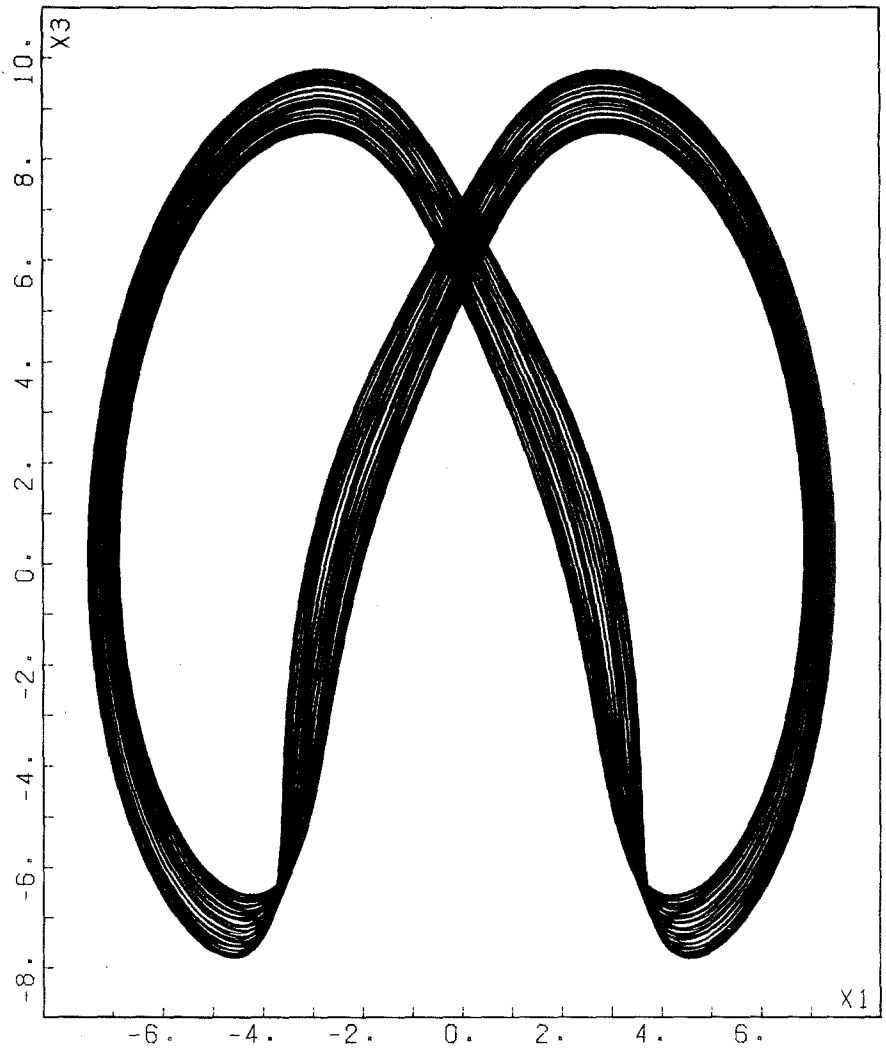

Fig. 6. Projections of the flow on a torus $T(\mathfrak{B})$ for $R = 196$.

initial point, which is attracted by a torus $T(\mathfrak{B})$, describes on it quasiperiodic trajectories, in the same way as we have seen for the two tori $T(\mathfrak{C})$. Figure 6 shows, for $R = 196$, a (x_1, x_3) projection of a point moving on a torus $T(\mathfrak{B})$: the solution curve appears to fill completely the torus. An analogous inference can be made looking at Fig. 7, showing for three different values of R a Poincaré map defined on the hyperplane $x_3 = 0$. For $R > R_{11}$ each torus $T(\mathfrak{B})$ does not attract any more, and any initial point, even if close to an orbit $\mathfrak{B}$, tends to a stable orbit $\mathcal{C}$ (see below).

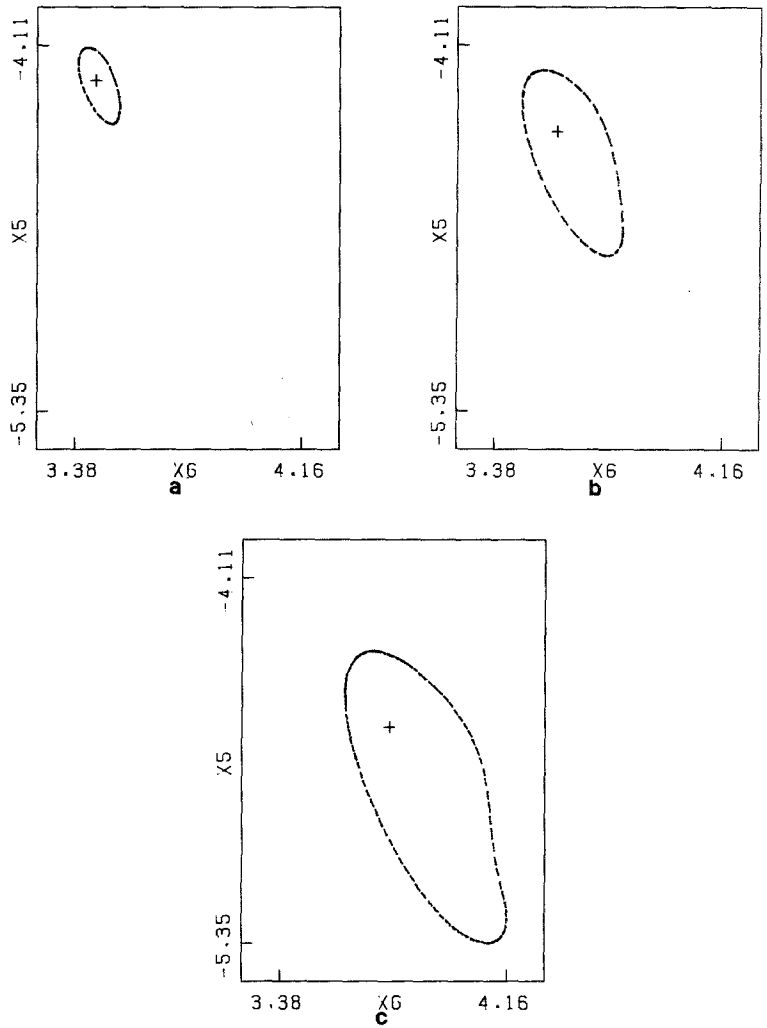

Fig. 7. Projections of a Poincaré map for the flow on a torus $T(\mathcal{B})$ on the hyperplane $x_3 = 0$ for $R =$ (a) 196 (100 intersections); (b) 210 (200 intersections); (c) 227 (400 intersections).

Consider now the bifurcation in R_3. Numerical computations show that such a bifurcation, unlike the one described above, is not a direct bifurcation to a torus T^2. In fact no attracting torus is present for $R < R_3$: for any initial point, arbitrarily close to an orbit $\mathcal{B}$, now unstable, the solution, after staying a long time in the neighborhood of $\mathcal{B}$, goes either to $\mathcal{C}_+$ or $\mathcal{C}_-$. It can then be reasonably hypothesized that in R_3 an inverted bifurcation to a torus T^2 takes place and that, for each orbit $\mathcal{B}$, an unstable torus exists, which shrinks to the orbit for R approaching R_3 from above.

We have followed the orbits B for $R < R_3$ and $R > R_{10}$, when they have become unstable. While for R decreasing the orbits soon become so unstable that it is impossible to follow them further on, for R increasing they have been followed much longer, up to $R = 800$.

4.3. ORBITS $\mathcal{C}$

For $141.7 \simeq R_6 < R < R_{12} \simeq 248.2$ two extra symmetric orbits $\mathcal{C}_1$ and $\mathcal{C}_2$ (Fig. 8) are present, stable and attracting, each one invariant under the symmetry (γ) and transformed in the other one by (α) or (β). The computation of the eigenvalues for the Poincaré map shows that one of them tends to cross the unit circle at $+1$ for R increasing towards R_{12}. It has been verified that the two orbits are not present any more for $R > R_{12}$ and that each one of them appears at $R = R_{12}$ together with an hyperbolic (unstable) one, in agreement with the bifurcation theory.

Looking at the stability properties of $\mathcal{C}_1$ and $\mathcal{C}_2$ for R decreasing, it has been found that they lose stability in R_6, when a pair of complex conjugate eigenvalues crosses the unit circle. It is easy to verify that, for R slightly smaller than R_6 and for any initial point arbitrarily close to an orbit $\mathcal{C}$, the solution goes to an orbit $\mathfrak{B}$, stable and attracting for this value of the parameter. As at $R = R_3$ for the orbits $\mathfrak{B}$, one can reasonably make the hypothesis of an inverted bifurcation to a torus T^2, even if numerical evidence for it cannot be given.

4.4. ORBITS $\mathfrak{D}$

For $146.61 \simeq R_8 < R < R_9 \simeq 166.59$ two symmetric orbits $\mathfrak{D}_1$ and $\mathfrak{D}_2$ (Fig. 9) are present, stable and attracting, each one invariant under the symmetry (α) and changed in the other one by (β) or (γ). The stability analysis of these orbits shows that both in R_8 and R_9 they become unstable because an eigenvalue of the Poincaré map leaves the unit circle through $+1$. In such a case the bifurcation theory[9] predicts that in generic conditions an orbit loses stability either exchanging it with another orbit present at the same time or, in presence of a symmetry, bifurcating to two new stable periodic orbits with breaking of the symmetry. However, neither of these is our case: all the many and careful numerical attempts looking for such an orbit at R_8 and R_9 were unsuccessful.

Following an orbit $\mathfrak{D}$, already unstable, for R decreasing, we were able to observe an interesting phenomenon: it disappears at $R = R_7 \simeq 142.97$ collapsing with another orbit "twice" unstable. In other words each orbit $\mathfrak{D}$ arises at $R = R_7$ already unstable, i.e., with an eigenvalue of the Liapunov matrix real and greater than $+1$.

As an attempt to interpret the bifurcations in R_7, R_8, and R_9, we think that the following hypothesis could be made: each orbit arises, at the same

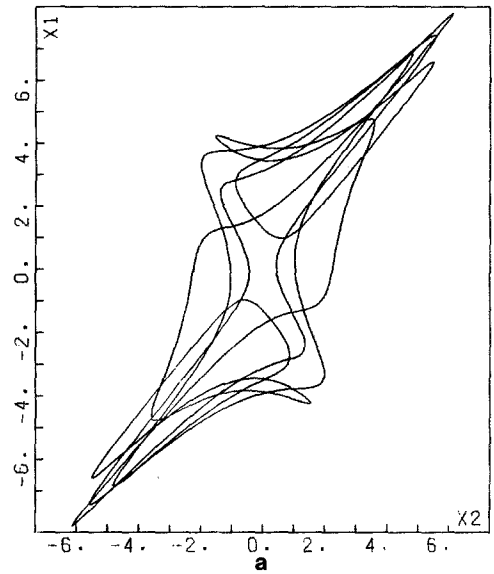

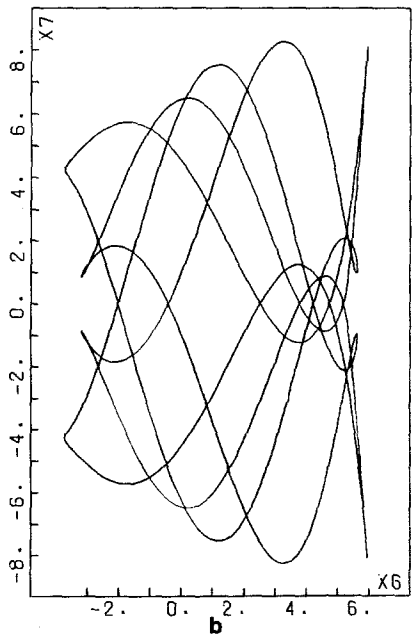

Fig. 8. Projections of a stable orbit $\mathcal{C}$ for $R = 200$.

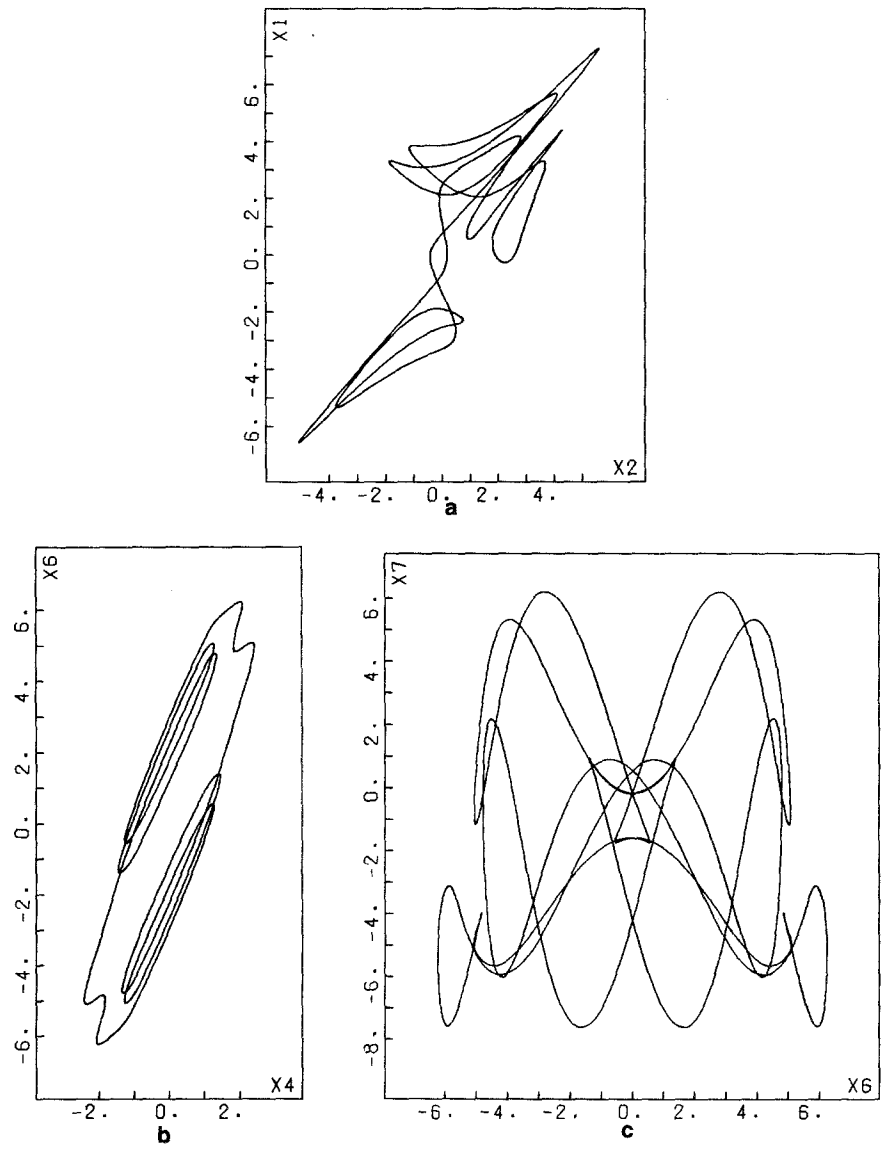

Fig. 9. Projections of a stable orbit $\mathfrak{O}$ for $R = 155$.

time with an hyperbolic one, on some invariant manifold which is unstable for $R = R_7$. As a consequence, the orbit is stable with respect to the manifold but unstable with respect to the full space. At $R = R_8$ that manifold, which might possibly be even a torus, becomes stable and attracting and with it also the orbit $\mathfrak{O}$. However the manifold, even if now

stable, is still "undetectable" because any numerical investigation shows only the orbit. At $R = R_9$ the manifold becomes unstable again and with it the orbit $\mathcal{D}$.

5. TURBULENCE

Consider now the behavior of system (2.2) for $R > R_{12}$, after each orbit $\mathcal{C}$ has disappeared collapsing with a hyperbolic one. No simple attractor is present: the three fixed points of (2.2) are unstable for quite a while; among all the closed orbits and tori previously described, trace is found of the unstable orbits $\mathcal{B}_1$ and $\mathcal{B}_2$ only.

By studying the flow of a randomly chosen initial point, trajectories are observed which all appear completely chaotic and sensitively dependent on initial conditions. For R not much greater than R_{12}, it is possible to observe that a significant role is still played by the unstable orbits $\mathcal{B}$. This appears clear if we look at Fig. 10a, showing a (x_4, x_5) projection of the flow of a random point for $R = 250$, and we compare it with Fig. 10b, showing for the same value of R the same projection of $\mathcal{B}_1$ and $\mathcal{B}_2$. Evidently the flow tends to become localized first in a neighborhood of an orbit $\mathcal{B}$, to spend some time there, and then to be pushed away to the neighborhood of the symmetric orbit $\mathcal{B}$. The entire process repeats itself indefinitely. This situation appears analogous to that found by Curry in Ref. 7, where the flow in the turbulent parameter range is driven by a similar mechanism, with two unstable tori replacing the two orbits $\mathcal{B}$. When R increases, the behavior of our system becomes more complicated (Fig. 11), appearing less influenced by the orbits $\mathcal{B}$, as they get more and more unstable.

Since all the numerical investigations carried on up to $R = 5000$ keep showing a stochastic behavior, we think that turbulence might also persist for R tending to infinity and no stable attracting periodic orbit exists at the high values of the Reynolds number.

6. CONCLUSIONS

In this work we have reported the results of our numerical investigation on a model of seven nonlinear ordinary differential equations. Such a model, obtained by a suitable seven-mode truncation of the Navier–Stokes equations for an incompressible fluid on a torus T^2, exhibits a very varied phenomenology, with an interesting sequence of bifurcations. Figure 12 shows a table which graphically summarizes the full behavior. It is straightforward to observe that four different and independent stories describe the complete phenomenology of the model. The first story consists of a sequence of bifurcations very similar to the one found by Curry in Ref. 7:

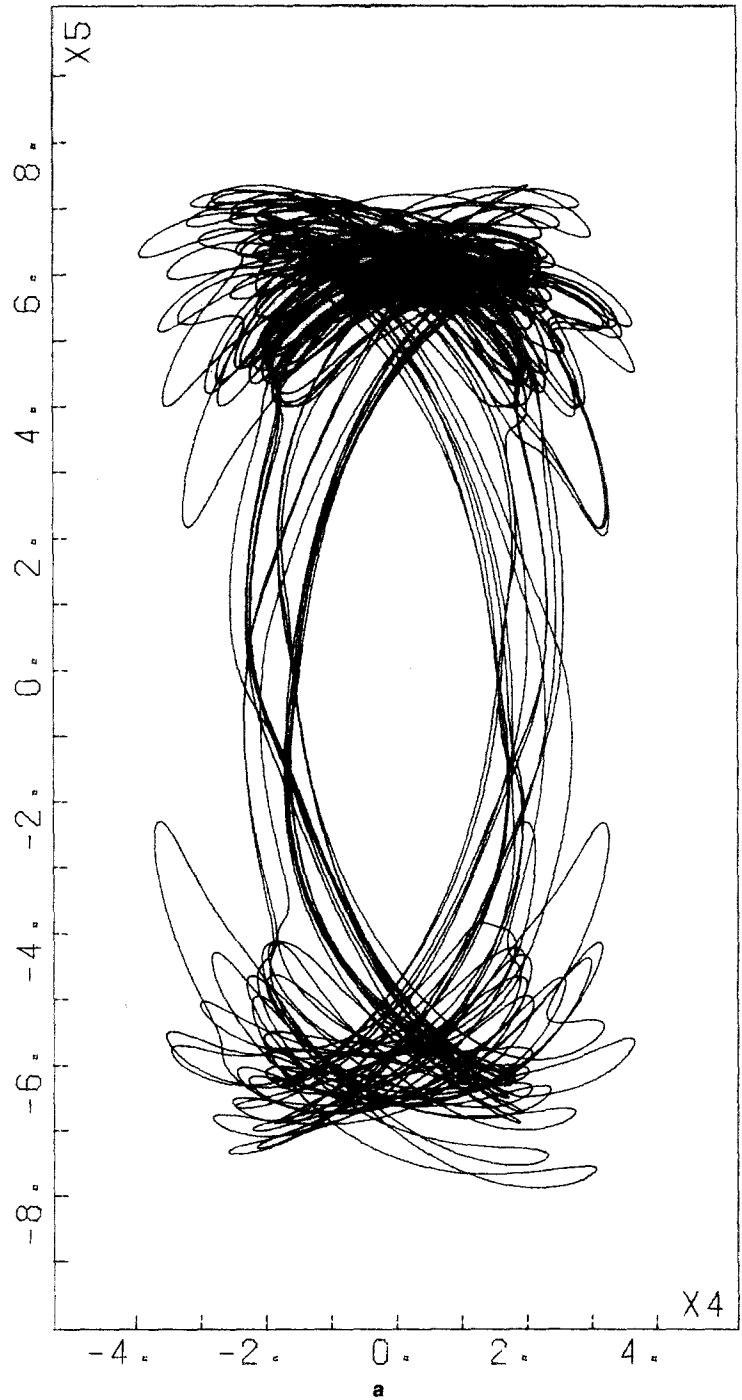

a

Fig. 10. (a) Projection of turbulent flow for $R = 250$; (b) Projection of the two unstable orbits $\mathfrak{B}$ for the same value of R.

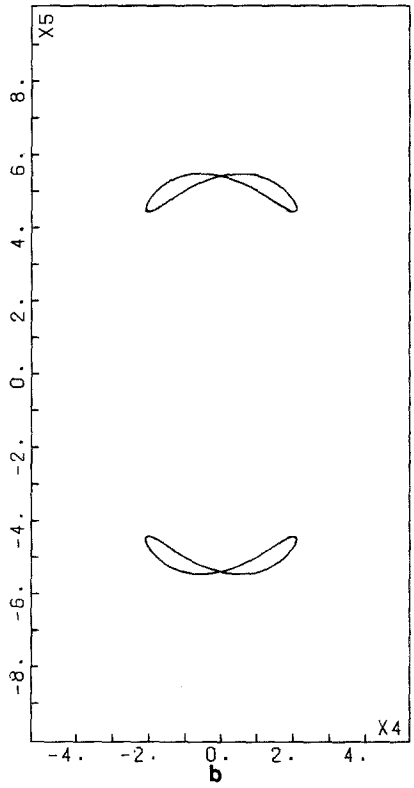

Fig. 10. Continued.

the fixed point P_0 bifurcates to the two fixed points P_+ and P_-; via a direct Hopf bifurcation P_+ and P_- bifurcate to the periodic orbits $\mathcal{C}_+$ and $\mathcal{C}_-$, which on their turn bifurcate to the tori $T(\mathcal{C}_+)$ and $T(\mathcal{C}_-)$. The further three stories, connected, respectively, to the existence of the orbits $\mathcal{B}$, $\mathcal{C}$, and $\mathcal{D}$, show three interesting examples of "life" of an orbit, each one with its own characteristics.

A remark which is also straightforward from the table in Fig. 11 concerns a strong phenomenon of hysteresis (i.e., coexistence of stable attractors) characterizing the model. In the interval (R_8, R_9) are present even three different stable orbits; in the intervals (R_4, R_5) and (R_{10}, R_{11}) hysteresis takes place between closed orbits and tori.

For all the values of the Reynolds number larger than R_{12}, when no stable periodic orbits or tori are present any more, the model exhibits a turbulent behavior. In fact any randomly chosen point describes trajectories which appear to be completely random and sensitively dependent on initial conditions.

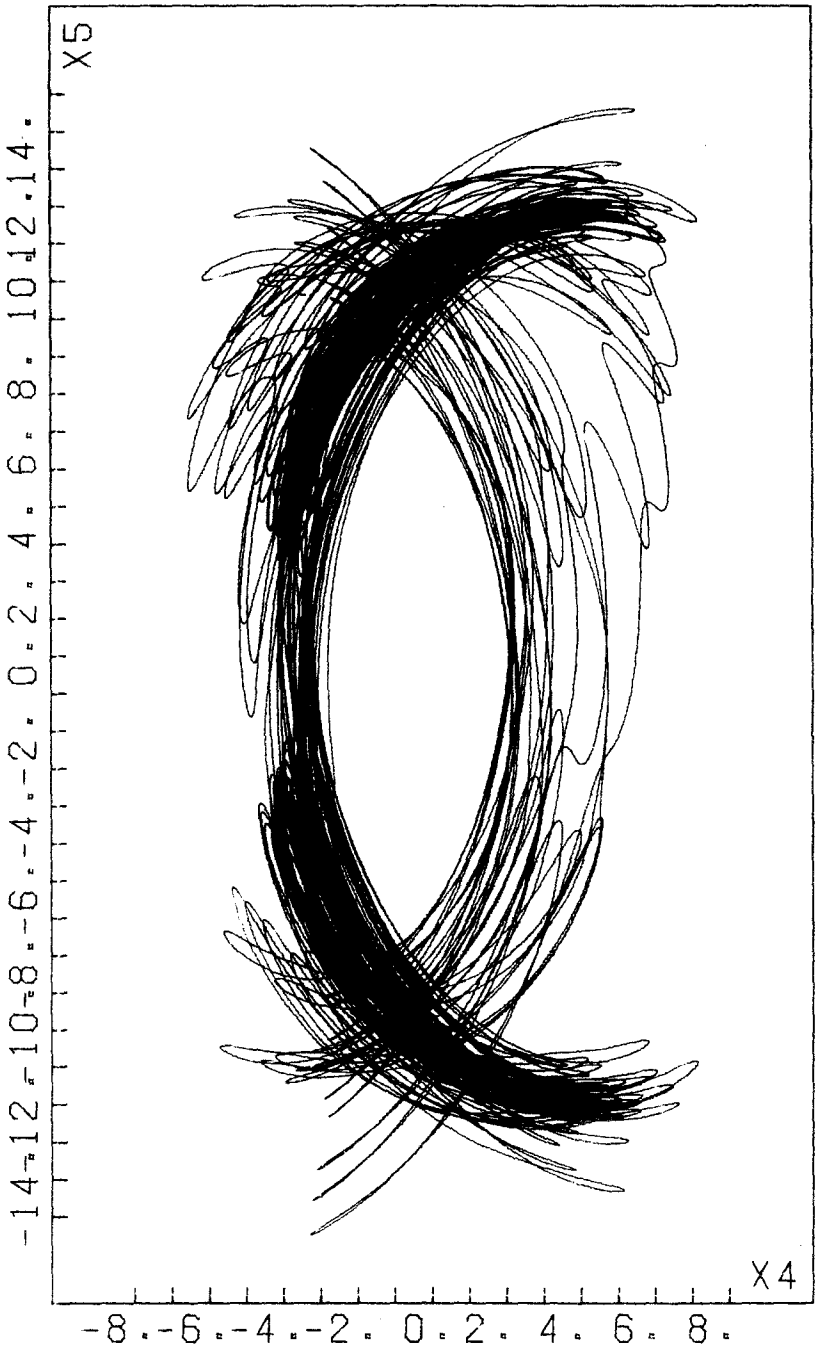

Fig. 11. Projection of turbulent flow for $R = 500$.

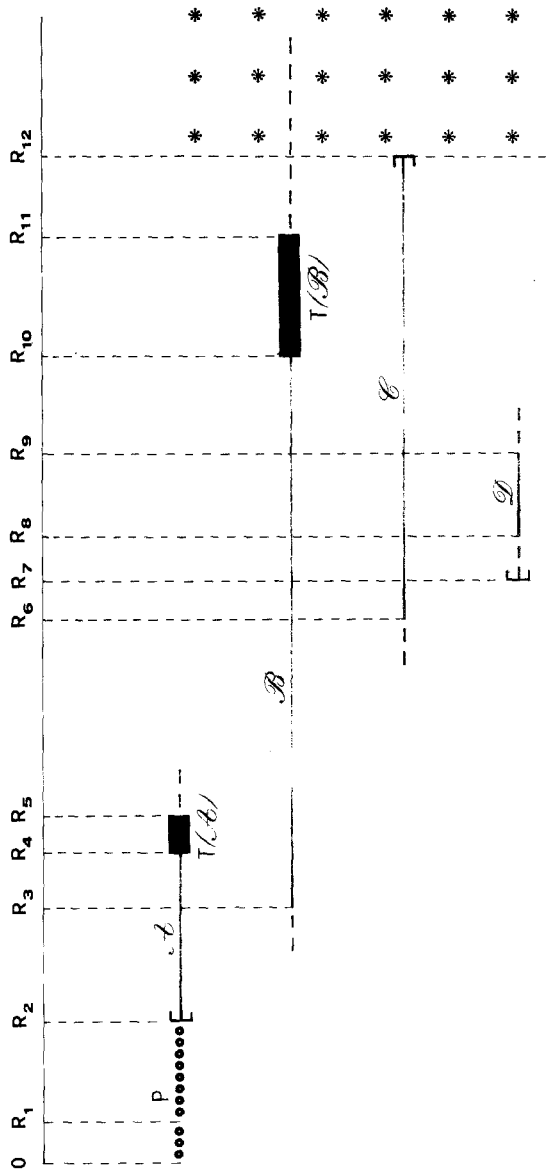

Fig. 12. Graphical summary of the phenomenology exhibited by system (2.2) as R varies. A sequence of ● indicates for that range of R a set of stable fixed points, a continuous line (——) a stable periodic orbit, a broken line (---) an unstable periodic orbit, a black "tube" (▬) an attracting torus T^2, a set of * turbulent regime.

As already observed in the Introduction, our seven-mode system does not reproduce the qualitative features of the five-mode model from which it has been obtained as an extension. This result makes more striking what appears already in Ref. 7, where a 14-mode generalization of the three-mode Lorenz system is presented: new modes can change quite completely the phenomenology of a model. At this point various questions arise naturally. Is it possible to explain how such a change happens? Is it a general property of truncated models or for large truncations is it possible to have a persistence in the qualitative phenomenology by addition of new modes? If the latter is the case is it reasonable to hope this will happen at a number of modes for which the model is still numerically analyzable? It is evident that for any attempt to answer these questions many more numerical investigations are still necessary, and perhaps not sufficient.

ACKNOWLEDGMENTS

We gratefully acknowledge many useful conversations with G. Gallavotti, whose continuous interest has been a strong support to our work.

REFERENCES

1. C. Boldrighini and V. Franceschini, *Commun. Math. Phys.* **64**:159 (1979).
2. V. Franceschini and C. Tebaldi, *J. Stat. Phys.* **21**:707 (1979).
3. D. Ruelle and F. Takens, *Commun. Math. Phys.* **20**:167 (1971).
4. E. N. Lorenz, *J. Atmos. Sci.* **20**:130 (1963).
5. K. A. Robbins, *SIAM J. Appl. Math.* **36**:457 (1979).
6. V. Franceschini, *J. Stat. Phys.* **22**:397 (1980).
7. J. H. Curry, *Commun. Math. Phys.* **60**:193 (1978).
8. O. A. Ladyzhenskaya, *The Mathematical Theory of Viscous Incompressible Flows* (Gordon and Breach, New York, 1969).
9. G. Iooss, *Bifurcation of Maps and Applications* (North-Holland, Amsterdam, 1979).